RSC Advances

ROYAL SOCIETY OF CHEMISTRY

www.rsc.org/advances

Cite this: DOI: 10.1039/c0xx00000x

www.rsc.org/xxxxxx

ARTICLE TYPE

Fabric-based flexible electrode with multi-walled carbon nanotubes@Ni network structure as a novel anode for hydrogen peroxide electrooxidation

Dongming Zhang, Dianxue Cao, Ke Ye, Yang Xu, Kui Cheng, Jinling Yin, Guiling Wang*

Received (in XXX, XXX) Xth XXXXXXXXX 20XX, Accepted Xth XXXXXXXXX 20XX
DOI: 10.1039/b000000x

A simple method involving dyeing and electrodeposition is introduced to fabricate a three-dimensional Ni@Multi-walled carbon nanotubes flexible electrode on wearable fabric. The as-prepared Ni@multi-walled carbon nanotubes/Fabric (Ni@MWNTs/Fabric) electrode is characterized by scanning electron microscope and X-ray diffraction spectrometer. The catalytic activity of the Ni@MWNTs/Fabric electrode for hydrogen peroxide electrooxidation is tested by means of cyclic voltammetry and chronoamperometry. Such a three demensional hybrid electrode structure allows a large specific surface area and a large mass loading, which lead to a high areal current density of 720 mA cm^{-2} at 0.5 V in 2 mol dm^{-3} NaOH and 2.5 mol dm^{-3} hydrogen peroxide. The electrode shows great promise as the anode of direct peroxide fuel cell due to its flexible, wearable, and environmentally friendly.

1. Introduction

Direct peroxide-peroxide fuel cell (DPPFC) has attracted much attention due to its low cost, compact, easy operation, workable without air, providing both power and oxygen, and so on [1-7]. As the anode fuel of DPPFC, the electrooxidation of hydrogen peroxide (H_2O_2) has fast kinetics and involve no poisoned species [1-13], which allows it a promising and environmentally friendly fuel. So the study of the electrocatalysts for H_2O_2 electrooxidation has become a hot topic in recent years. Several types of catalysts for the electrooxidation of H_2O_2 have been developed. It is reported that previous metals, such as platinum [4, 8-10], palladium [4, 5], gold [4-5, 11], silver [12] and a combination of these [5] exhibit effective catalytic performance, but the high prices and the limited resource restrict their extensive utilization. In order to cut down the use amount of noble metals and reduce the cost of electrode, transition metals, such as Ni, Co [4, 6, 7], are employed to catalyze the H_2O_2 electrooxidation. However, they suffer a drawback of low catalytic activity. So, developing the transition catalysts, which can make H_2O_2 electrooxidation more effective, is necessary and meaningful.

An excellent substrate is one of the decisive factors that determine a catalytic activity of an electrode. And then, the structure, conductivity, mechanical stability and price are the considerations that judge whether the collector is a promising material to apply to our daily life and industrial production. Metallic materials (e.g. aluminum foil, titanium plate, copper sheet) [14-19] are the most widely used electrode material due to its high electronic conductivity. Nowadays, carbon materials (e.g. carbon cloth, carbon paper) [5-6, 20-22] are usually as the collector due to their deformability. Recently, three dimensional (3D) structure electrodes (e.g. nickel foam, copper foam, titanium foam, sponge and some other foams and nano wires) [7, 23-30] have become a research hotspot owing to their excellent mass transport property, high catalyst utilization and capability of achieving large catalytic surface areas. Nowadays, energy storage devices based on conductive paper [31] or textile [32] with carbon nanotubes (CNTs) has attracted much attention. However, few of them have been employed as a flexible electrode substrate for DPPFC.

Fabrics, which are the raw material of clothes, towels, bed sheets, cotton pads, is indispensable in our daily life. In general, these fabrics are abandoned after the use of a period of time, which will lead to a waste of resource and environmental pollution. Almost all of the people ignore this phenomenon.

In this work, we fabricated a novel MWNTs/Fabric substrate by a simply "dipping and drying" method. The fabric is the cotton pads disused by a girl. MWNTs were wrapped around the fabric by Van der Waals forces and the MWNTs/Fabric exhibits a unique 3D network structure compared with the carbon cloth and carbon paper. Nano-scaled Ni particles were electrodeposited on the surface of the MWNTs/Fabric. The Ni@MWNTs/Fabric electrode saves the metal resources of the electrode material compared with the conventional metal electrode and shows a remarkably high catalytic activity for H_2O_2 electrooxidation. Besides, the MWNTs/Fabric is much cheaper than the carbon cloth and the utilization of the discarded fabrics reduces environmental pollution.

2. Experimental

Fabrication:

The MWNTs/Fabric substrate is prepared by self-assembling of

MWNTs' layer on a fabric. The fabric is the disused cotton pads, which is commercially made up of polyester fibers and has a high hygroscopicity as a normal cloth (HAOLING Daily necessily & Cosmetics Co. Ltd.). In detail, a piece of fabric were first washed by acetone and ethanol for several times and then dried at 373.15 K in a vacuum oven for 2 hours prior to use. Then the cleaned fabric was dipped into a ultrasonic uniform suspension that contains 0.13 g MWNTs (> 50 nm in outer diameter and 10-20 μm in length, Shenzhen Nanotech Port Co. Ltd.), 0.5 g sodium dodecyl benzene sulfonate (SDBS) and 50 mL ultrapure water (Milli-Q, 18 MΩ cm). After dipping for 30 s, the fabric was removed from the suspension and dried at 373.15 K for 2 hours. The dip-dry cycle was repeated 5 times to obtain the MWNTs/Fabric substrate, which were further washed with a large amount of ultrapure water to remove SDBS. The Ni@MWNTs/Fabric electrode was prepared by electrodeposition of Ni on the surface of the MNWNs/Fabric, which was carried out in a standard three-electrode electrochemical cell using a computerized potentiostat (Autolab PGSTAT302, Eco Chemie) controlled by GPES software. A piece of MWNTs/Fabric substrate (10×10 mm) was employed as the working electrode, a platinum foil as the counter electrode, and a saturated Ag/AgCl, KCl electrode as the reference electrode. The electrodeposition were carried out at a constant current of 5, 10, 15 and 20 mA cm^{-2} in 2 mol dm^{-3} NH_4Cl and 0.1 mol dm^{-3} $NiCl_2$, respectively. The electrodeposition time was kept constant at 4 hours.

Materials characterization:

The morphology of the electrodes was determined using a scanning electron microscope (SEM, JEOL JSM-6480). The structure was analyzed by a powder X-ray diffractometer (XRD, Rigaku TTR- III) equipped with Cu Kα radiation (λ=0.15406 nm).

Electrochemical measurements:

The electrochemical oxidation of H_2O_2 was measured by cyclic voltammetry and chronoamperometry in the same three-electrode electrochemical cell using NaOH as the electrolyte and the 1cm^2 Ni@MWNTs/Fabric electrode. All solutions were made with analytical grade chemical reagents and ultra-pure water (Milli-Q 18 MU cm). All potentials were referred to the saturated Ag/AgCl, KCl reference electrode.

3. Results and discussion

The fabrication process of the Ni@MWNTs/Fabric electrode via dyeing and electrodeposition is illustrated in Fig. 1. The original fabric is pure white, and after dyeing of MWNTs and electrodeposition of Ni, the fabric becomes black and green, respectively. The MWNTs/Fabric substrate is about 0.0079 g and the mass reached to 0.0155, 0.0228, 0.0272 and 0.0304 g after 4 h electrodeposition at the constant current densities of 5, 10, 15 and 20 mA cm^{-2}, respectively. The SEM images of the bare MWNTs/Fabric and the Ni@MWNTs/Fabric electrode prepared at different electrodeposition current density (5, 10, 15, 20 mA cm^{-2}) are shown in Fig. 2. At low magnification, it is obvious that the MWNTs/Fabric substrate, constituted by fabric lines (Fig. 2a), exhibits a 3D-network structure. The diameter of the single fabric liner is around 15 μm. At high magnification, we found that the single fabric line is comprised by some detailed-lines (Fig. 2b). The fabric line shows a plush stuffed surface, which indicated that the MWNTs were coated in the surface. The existence of MWNTs ensures good electrical conductivity (A sheet resistance of 1Ω/square, measured by four points probe technique) of the MWNTs/Fabric substrate. Besides, the H_2O_2 can be absorbed by the fabric, which ensures a full contact between the H_2O_2 and Ni during the reaction process. The surface of the fabric lines are encapsulated by the Ni after the electrodeposition process (Fig. 2c, e, g, i). In order to compare the Ni particles in the surface of the fabric line at different electrodeposition current densities (5, 10, 15, 20 mA cm^{-2}), the detail of the four kinds electrodes surfaces are shown by Fig. 2d, f, h and j. As depicted in the figures, the diameters of the Ni particles prepared at 5 and 10 mA cm^{-2} are around 1100 nm and the diameter is over 1200 nm when the electrodeposition current density reached to 20 mA cm^{-2}. However, the diameters of the Ni particles prepared at 15 mA cm^{-2} are only around 700 nm. First, the diameter of the Ni nanoparticles is determined by the overpotential. When the overpotential increases, the diameter of the Ni nanoparticles will decrease. With the increase of the current density, the overpotential increases. So the diameter of the Ni nanoparticles electrodeposited in 15 mA cm^{-2} is smaller than them at 5 and 10 mA cm^{-2}. However, when the electrodeposition is over high (20 mA cm^{-2}), the electric quantity is higher than the other conditions and the electrodeposition mount of the metallic Ni is more than the other conditions (5, 10, 15 mA cm^{-2}), which is further demonstrated by the electrodeposition mass of the Ni particles (Fig. 1). Second, the metallic Ni is ferromagnetic and the massive Ni particles will aggregate at 20 mA cm^{-2}, which lead to a bigger diameter of Ni particles. So the Ni electrodes prepared at 15 mA cm^{-2} exhibits the largest specific surface area. This will remarkably increase the activity of the Ni owning to the highest surface energy than others.

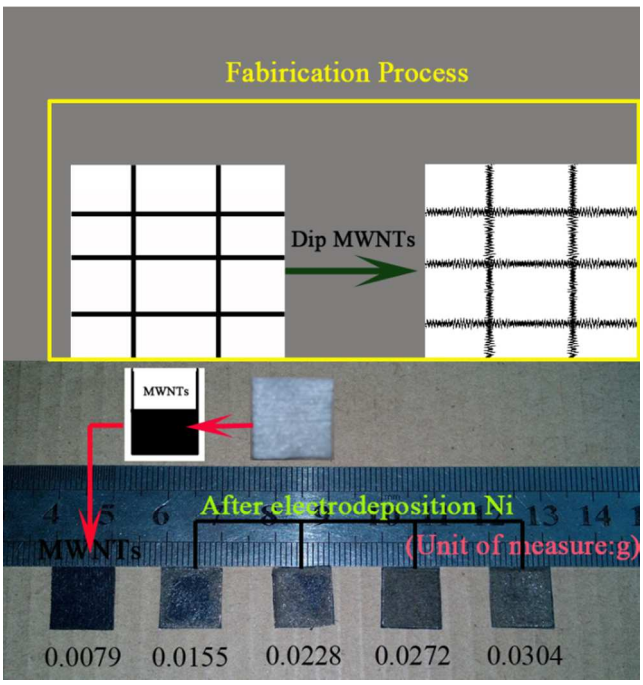

Fig. 1 Fabrication process of the Ni@MWNTs/Fabric electrode.

The X-ray diffraction patterns of the Ni@MWNTs/Fabric electrodes are shown in Fig. 3. The scan range was set from 10° to 85° . It is obvious that the diffraction peaks between 15° to 30° are the substrate peaks. According to the JCPDS card No. 04-8450, the (1 1 1), (2 0 0), (2 2 0) diffractions of cubic Ni are located at 2θ=44°, 52°, 76°, respectively. It demonstrates that Ni presents in a metallic state of oxides or hydroxides. The intensity of the three Ni peak increases with increase of the electrodeposition current density, so it indicates that the content of the Ni in the Ni@MWNTs/Fabric increases.

The H_2O_2 electrooxidation activities on the Ni@MWNTs/Fabric electrode with different electrodeposition current density are shown in Fig. 4. Fig. 4a to d represents the electrodeposition current densities range from 5 to 20 mA cm^{-2}. All of the open circuit potentials (OCP) of the Ni@MWNTs/Fabric electrode in H_2O_2 solution are around – 0.16 V. The Ni@MWNTs/Fabric electrode exhibits a strong oxidation peak at around 0.43 V and an obvious reduction peak at around 0.23 V in blank NaOH solution, which is attributed to the redox reactions of Ni^{2+}/Ni^{3+} according to the previous report [4, 6-7]. The surface of the metallic Ni will be partly oxidized to Ni^{2+} in a solution with strong oxidization and the conversion of Ni^{2+}/Ni^{3+} will occur at high potential. Besides, the existence of Ni^{2+} helps the negative valence oxygen in H_2O_2 to diffuse to the surface of the Ni electrode. Compared with the electrooxidation behavior in bare NaOH solution, the current density at the oxidation peak increases with the increase of the H_2O_2 solution, which demonstrated that the oxidation of H_2O_2 is controlled by diffusion at low H_2O_2 concentration. When the H_2O_2 concentration is higher than 1.0 mol dm^{-3}, the oxidation peak of H_2O_2 disappeared. The highest current density at 0.5 V as a function of the deposition current density is shown in fig. 4e. Clearly, the highest oxidation current density reached to 340, 630, 720 and 640 mA cm^{-2} at 0.5 V in 2.0, 3.5, 2.5 and 3.0 mol dm^{-3} H_2O_2 solution on the four electrodes. But if the H_2O_2 concentration increases further, the current density will decrease.

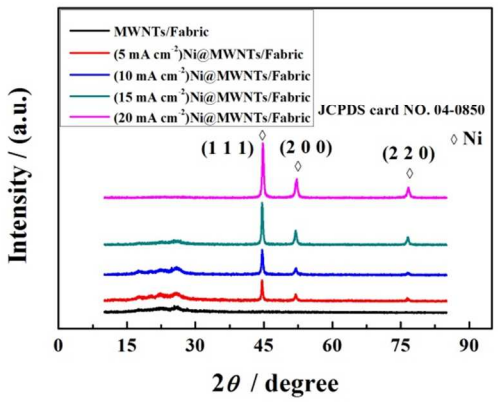

Fig. 3 X-ray diffraction patterns of the Ni@MWNTs/Fabric electrodes.

The schematic diagram depicting the mechanism for the H_2O_2 electrooxidation on the Ni@MWNTs/Fabric electrode is illustrated by Fig. 5. The catalytic performance of electrooxidation of H_2O_2 on the electrode is effect seriously by H_2O_2 concentration. When H_2O_2 concentration is low, there are adequate Ni particles acted as the catalytic sites for H_2O_2 electrooxidation, the O-O bond can be fully contacted with Ni (style Ⅰ in Fig. 5) and convert to O_2 and release electrons [eq.1] (2-8). With increasing the H_2O_2 concentration, all of the catalytic sites in Ni particles will be occupied by O-O bond and some surplus H_2O_2 can't be electro-catalyzed (style Ⅱ in Fig. 5). However, when the H_2O_2 concentration is over high, most of the O-O bond in H_2O_2 can't come into contact with Ni, which will cause a large number of hydrolysis of H_2O_2 [eq.2] (style Ⅲin Fig. 5) (2-5), and the released O_2 will be adsorbed on the surface of the Ni particles and inhibit the contact between the Ni and H_2O_2. Besides, the released O_2 may reduce the electronic conductivity of the reaction solution, which will also lead a poor performance.

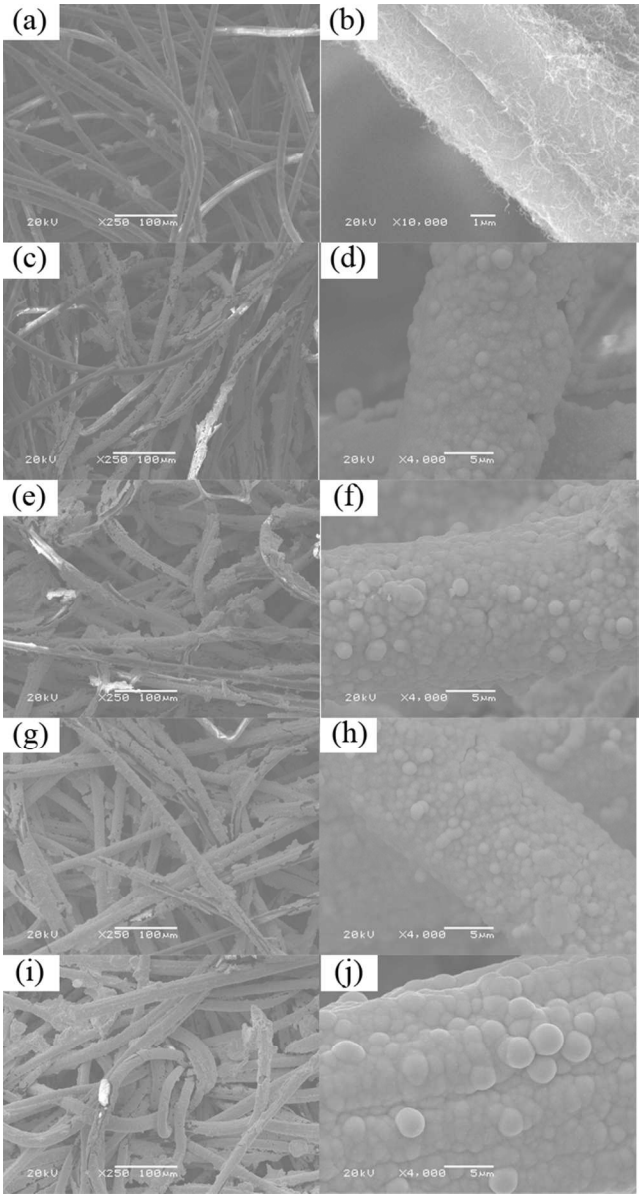

Fig. 2 SEM images of the bare MWNTs/Fabric (a, b) and the Ni@MWNTs/Fabric electrode prepared at different electrodeposition current density 5 (c, d), 10 (e, f), 15 (g, h), 20 (i, j) mA cm^{-2}

When the concentration of the alkali liquor was fixed, the H_2O_2 at high concentration (0.25~2.0 mol dm^{-3}) almost have none influence for the electrooxidation of H_2O_2 on the Ni-carbon fiber

[6] and Ni-Ni foam [7] electrodes. However, the catalytic performance of the H_2O_2 electrooxidation is remarkably affected by the H_2O_2 concentration (0.20~2.5 mol dm^{-3}) on the Ni@MWNTs/Fabric electrode, which is vital to change discharge current to satisfy industrial requirements. So as the fuel of the underwater and space power source, the H_2O_2 at high and different concentration not only can provide large amounts of oxygen for breathing and offer different discharge current, both of which is more favorable than our previous work [6-7].

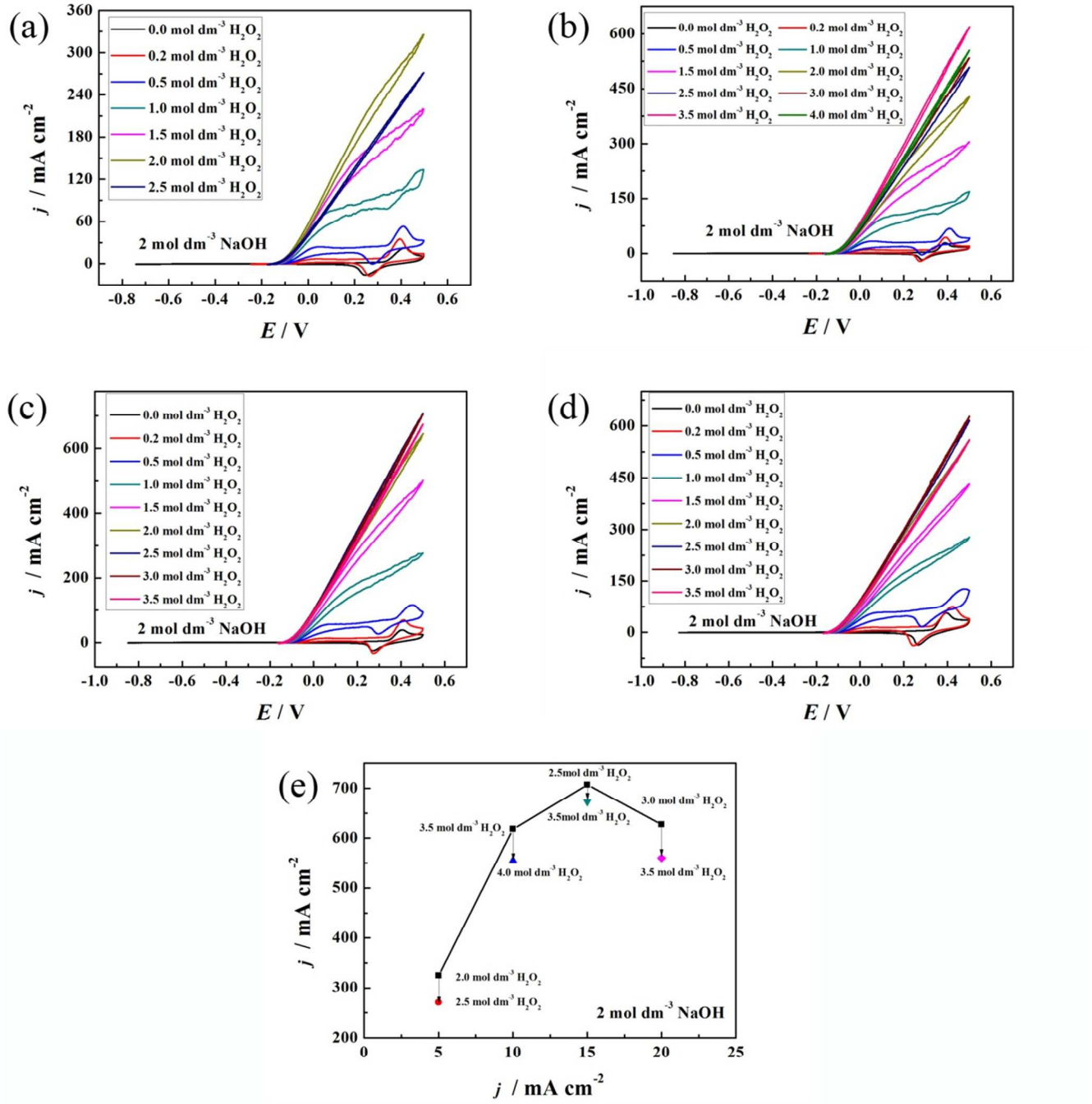

Fig. 4 H_2O_2 electrooxidation activities on the Ni@MWNTs/Fabric electrode with different electrodeposition current density a) 5 mA cm^{-2}, b) 10 mA cm^{-2}., c) 15 mA cm^{-2}, d) 20 mA cm^{-2}, Scan rate: 50 mV s^{-1}. The highest current density at 0.5 V as a function of the deposition current density (e)

$$H_2O_2 + 2OH^- \rightarrow 2H_2O + O_2 + 2e^- \quad (1)$$

$$2H_2O_2 \rightarrow 2H_2O + O_2 \quad (2)$$

Among the four electrodes, the highest catalytic performance is the electrode prepared at a constant electrodeposition current of 15 mA cm^{-2} (Fig. 4e), so we discussed the specific catalytic activity of H_2O_2 electrooxidation on this electrode in the following work.

The effects of NaOH concentration are discussed in Fig. 6. The concentration of H_2O_2 was fixed at 1.0 mol dm^{-3} and the concentration of NaOH varies from 1 to 6 mol dm^{-3}. All of the onset potentials are around – 0.16 V. At low NaOH concentrations (1 and 3 mol dm^{-3}), the current density reached to around 270 mA cm^{-2} and there is no obvious reduction peak in the CV curves. As contrast, the reduction peaks gradually shifted to the negative direction when the NaOH concentration increases from 3 to 6 mol dm^{-3}. Clearly, the current densities decrease significantly when the concentration of NaOH is higher than 3 mol dm^{-3}. The over high NaOH concentration reduces the H_2O_2 concentration that diffuse to the surface of the electrode. Besides, it is obvious that the MWNTs/Fabric has no catalytic activity for the H_2O_2 electrooxidation.

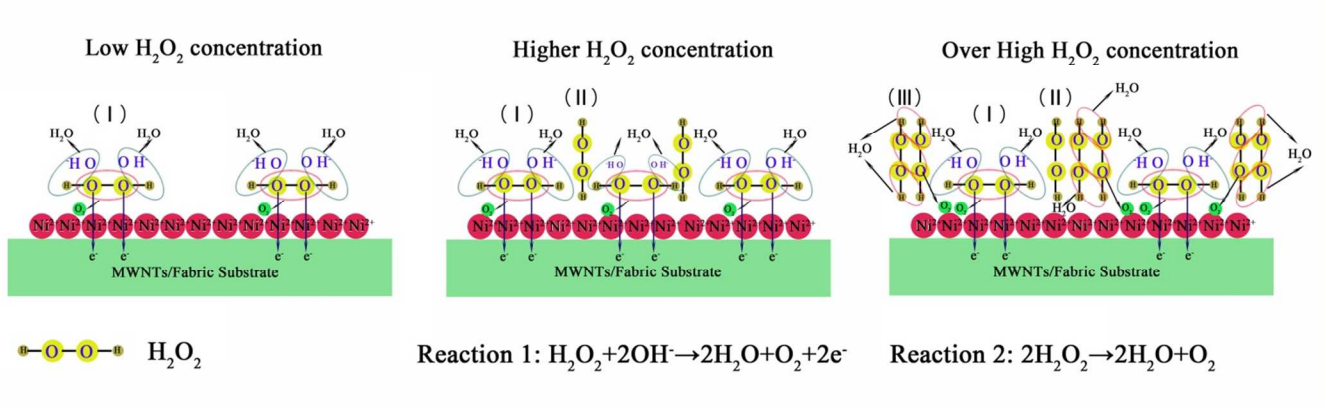

Fig. 5 Schematic diagram depicting the mechanism for the H_2O_2 electrooxidation on the Ni@MWNTs/Fabric electrode.

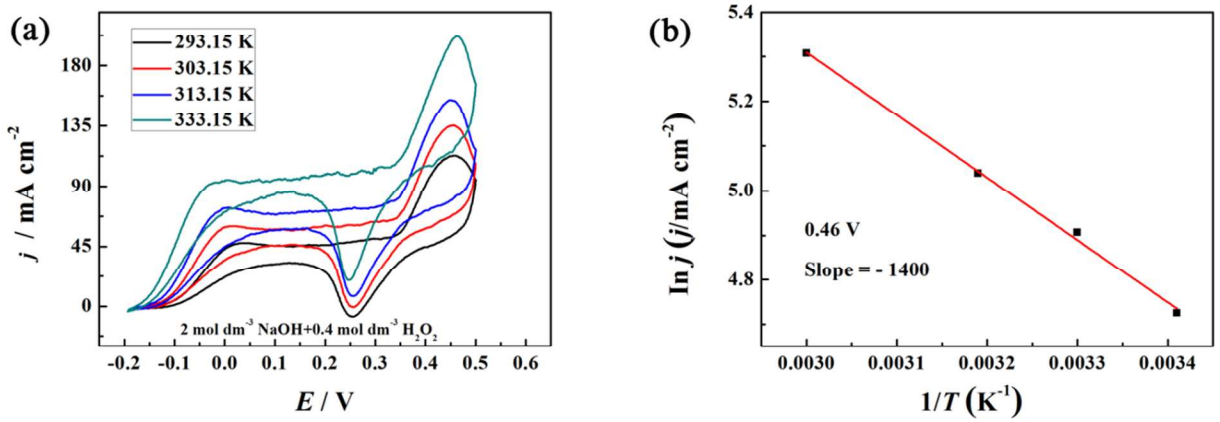

Fig. 8 The cyclic voltammograms of H_2O_2 electrooxidation on the Ni@MWNTs/Fabric electrode in 2.0 mol dm^{-3} NaOH and 0.4 mol dm^{-3} H_2O_2 at different temperatures, Scan rate: 50 mV s^{-1} (a); Arrhenius plot of the current densities at 0.46 V for H_2O_2 electrooxidation on the Ni@MWNTs/Fabric electrode (b).

The stability of Ni@MWNTs/Fabric electrode for H_2O_2 electrooxidation was investigated by chronoamperometric measurements in 2 mol dm^{-3} NaOH and 2.0 mol dm^{-3} H_2O_2. The result is shown in Fig. 7. The potentials were selected in the region according to the polarization curves in Fig. 4. At low potentials (-0.05 V and 0.05 V), the oxidation current density reached to steady-state quickly after about 50 s and kept stable during the 20 min test period. However, when the constant potential was applied at 0.15 V, the CA curve gets rough and the current density decreased slightly during the reaction process. This phenomenon may be caused by the large amount of oxygen bubbles in the surface of electrode and the consumption of the H_2O_2 at high oxidation potential [7].

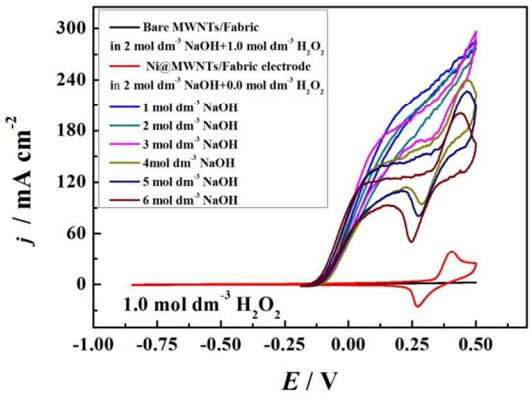

Fig. 6 The cyclic voltammograms for the Ni@MWNTs/Fabric electrode in x mol dm^{-3} NaOH (x=1, 2, 3, 4, 5, 6) and 1.0 mol dm^{-3} H_2O_2; the bare MWNTs/Fabric in 2 mol dm^{-3} NaOH and 1.0 mol dm^{-3} H_2O_2 and the Ni@MWNTs/Fabric electrode in 2 mol dm^{-3} NaOH and 0.0 mol dm^{-3} H_2O_2 are also shown for comparison, Scan rate: 50 mV s^{-1}.

The reaction temperature has great influence on the electrochemical behavior of H_2O_2 electrooxidation. It can be seen from Fig. 8, the onset potentials move a little more negatively and the oxidation current densities increase obviously with increasing the temperature, respectively (Fig. 8a). The activation energy for the electrooxidation of H_2O_2 on Ni@MWNTs/Fabric electrode was calculated to be -11.64 KJ mol^{-1} obtained from the Arrhenius relationship (Eq. 3) [7]. Where j is the current density; T is the thermodynamic temperature; R is the molar gas constant; and Ea is the activation energy. The logarithm of peak current densities (ln j) at 0.46 V were plotted against the reciprocal of absolute temperatures (1/T) (Fig. 8b).

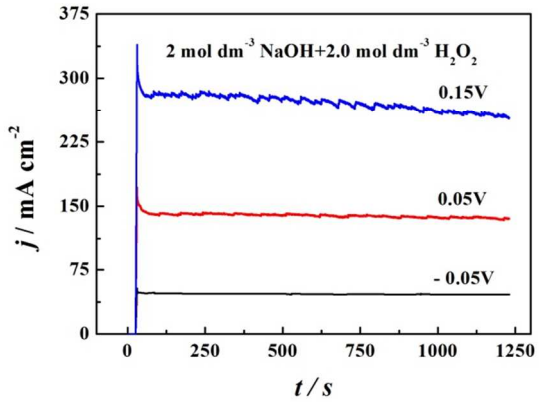

Fig. 7 Chronoamperometric curves for H_2O_2 electrooxidation at different potentials in 2.0 moldm^{-3} NaOH and 2.0 mol dm^{-3} H_2O_2.

$$\frac{\partial \ln j}{\partial T} = \frac{E_a}{RT^2} \quad (3)$$

4. Conclusions

In summary, a novel Ni@MWNTs/Fabric electrode, assembled by simple directly infiltrating and electrodeposition methods, is employed to catalyze the electrooxidation of H_2O_2. The Ni@MWNTs/Fabric electrode exhibits a 3D network structure and allows a large mass loading of Ni particles. The oxidation current density reached to 720 mA cm^{-2} in 2.0 mol dm^{-3} NaOH and 2.5 mol dm^{-3} H_2O_2 at 0.5 V. The activation energy for the electrooxidation of H_2O_2 on Ni@MWNTs/Fabric electrode was calculated to be -11.64 KJ mol^{-1}.

Acknowledgments

We gratefully acknowledge the finance supported by the Fundamental Research Funds for the Central Universities (HEUCF20130910013).

Notes and references

Key Laboratory of Superlight Materials and Surface Technology of Ministry of Education, College of Materials Science and Chemical Engineering. Harbin Engineering University, Harbin, 150001, P.R.China. E-mail: wangguiling@hrbeu.edu.cn*; Fax: +010-86-451-82589036; Tel: +010-86-451-82589036*

[1] S.A. Mousavi Shaegh, N.-T. Nguyen, S.M. Mousavi Ehteshami, S.H. Chan, A membraneless hydrogen peroxide fuel cell using prussian blue as cathode material, Energy & Environmental Science 5 (2012) 8225.

[2] Y. Yamada, S. Yoshida, T. Honda, S. Fukuzumi, Protonated iron–phthalocyanine complex used for cathode material of a hydrogen peroxide fuel cell operated under acidic conditions, Energy & Environmental Science 4 (2011) 2822.

[3] Y. Yamada, Y. Fukunishi, S.-i. Yamazaki, S. Fukuzumi, Hydrogen peroxide as sustainable fuel: electrocatalysts for production with a solar cell and decomposition with a fuel cell, Chemical Communications 46 (2010) 7334.

[4] S.-i. Yamazaki, Z. Siroma, H. Senoh, T. Ioroi, N. Fujiwara, K. Yasuda, A fuel cell with selective electrocatalysts using hydrogen peroxide as both an electron acceptor and a fuel, Journal of Power Sources 178 (2008) 20.

[5] F. Yang, K. Cheng, T. Wu, Y. Zhang, J. Yin, G. Wang, D. Cao, Dendritic palladium decorated with gold by potential pulse electrodeposition: Enhanced electrocatalytic activity for H_2O_2 electroreduction and electrooxidation, Electrochimica Acta 99 (2013) 54.

[6] F. Yang, K. Cheng, X. Xiao, J. Yin, G. Wang, D. Cao, Nickel and cobalt electrodeposited on carbon fiber cloth as the anode of direct hydrogen peroxide fuel cell, Journal of Power Sources 245 (2014) 89.

[7] F. Yang, K. Cheng, X. Xue, J. Yin, G. Wang, D. Cao, Three-dimensional porous Ni film electrodeposited on Ni foam: High performance and low-cost catalytic electrode for H_2O_2 electrooxidation in KOH solution, Electrochimica Acta, 107 (2013) 194.

[8] S.B. Hall, E.A. Khudaish, A.L. Hart, Electrochemical oxidation of hydrogen peroxide at platinum electrodes. Part 1. An adsorption-controlled mechanism, Electrochimica Acta 43 (1997) 579.

[9] S.B. Hall, E.A. Khudaish, A.L. Hart, Electrochemical oxidation of hydrogen peroxide at platinum electrodes. Part II: effect of potential, Electrochimica Acta 43 (1998) 2015.

[10] S.B. Hall, E.A. Khudaish, A.L. Hart, Electrochemical oxidation of hydrogen peroxide at platinum electrodes. Part III: Effect of temperature, Electrochimica Acta 44 (1999) 2455.

[11] M. Gerlache, Z. Senturk, G. Quarin, J.-M. Kauffmann, Electrochemical Behavior of H_2O_2 on Gold, Electroanalysis 9 (1997) 1088.

[12] M. Honda, T. Kodera, H. Kita, On the electrochemical behavior of H_2O_2 at Ag in alkaline solution, Electrochimica Acta 28 (1983) 727.

[13] A. Aytaç, M. Gürbüz, A.E. Sanli, Electrooxidation of hydrogen peroxide and sodium borohydride on Ni deposited carbon fiber electrode for alkaline fuel cells, International Journal of Hydrogen Energy 36 (2011) 10013.

[14] C. Iwakura, Y. Fukumoto, H. Inoue, S. Ohashi, S. Kobayashi, H. Tada, M. Abe, Electrochemical characterization of various metal foils as a current collector of positive electrode for rechargeable lithium batteries, Journal of Power Sources 68 (1997) 301.

[15] H.-C. Wu, E. Lee, N.-L. Wu, T.R. Jow, Effects of current collectors on power performance of $Li_4Ti_5O_{12}$ anode for Li-ion Battery, Journal of Power Sources 197 (2012) 301.

[16] S.-L. Sin, L.-L. Teo, K.-S. Tan, C.-Y. Chan, ESCA and TOF-SIMS study on oxidised and reduced polypyrrole-poly(4-styrenesulfonate) free-standing films synthesized on Ti electrodes, Electrochemistry Communications 2 (2000) 685.

[17] G. Wang, Y. Lin, Performance characteristics of dye-sensitized solar cells with counter electrode based on NiP-plated glass and titanium plate, Current Applied Physics 9 (2009) 1005.

[18] G. Fonder, C. Volcke, B. Csoka, J. Delhalle, Z. Mekhalif, Electrochemical and spectroscopic study of $C_{12}H_{25}X$ molecules adsorption on copper sheets, X (–SH, –S–S–, –SeH and –Se–Se–), Electrochimica Acta 55 (2010) 1557.

[19] X.H. Huang, X.H. Xia, Y.F. Yuan, F. Zhou, Porous ZnO nanosheets grown on copper substrates as anodes for lithium ion Batteries, Electrochimica Acta 56 (2011) 4960.
[20] A. Perrard, L. Retailleau, R. Berjoan, J.-P. Joly, Liquid phase oxidation kinetics of an excellulose activated carbon cloth by NaOCl, Carbon 50 (2012) 2226.
[21] M.-C. Tsai, T.-K. Yeh, Z.-Y. Juang, C.-H. Tsai, Physical and electrochemical characterization of platinum and platinum–ruthenium treated carbon nanotubes directly grown on carbon cloth, Carbon 45 (2007) 383.
[22] Q. Si, M. Kawakubo, M. Matsui, T. Horiba, O. Yamamoto, Y. Takeda, N. Seki, N. Imanishi, Silicon-carbon composite dispersed in a carbon paper substrate for solid polymer lithium-ion batteries, Journal of Power Sources 248 (2014) 1275.
[23] N. Feng, D. Hu, P. Wang, X. Sun, X. Li, D. He, Physical Chemistry Chemical Physics, 15 (2013) 9924.
[24] K. Ji, C. Xu, H. Zhao, Z. Dai, Electrodeposited lead-foam grids on copper-foam substrates as positive current collectors for lead-acid batteries, Journal of Power Sources 248 (2014) 307.
[25] X. Niu, Y. Li, J. Tang, Y. Hu, H. Zhao, M. Lan, Electrochemical sensing interfaces with tunable porosity for nonenzymatic glucose detection: A Cu foam case, Biosensors and Bioelectronics 51 (2014) 22.
[26] Z. Bi, M.P. Paranthaman, P.A. Menchhofer, R.R. Dehoff, C.A. Bridges, M. Chi, B. Guo, X.-G. Sun, S. Dai, Self-organized amorphous TiO_2 nanotube arrays on porous Ti foam for rechargeable lithium and sodium ion batteries, Journal of Power Sources 222 (2013) 461.
[27] W. Chen, R.B. Rakhi, L. Hu, X. Xie, Y. Cui, H.N. Alshareef, High-performance nanostructured supercapacitors on a sponge, Nano Letters 11 (2011) 5165.
[28] W. Chen, R.B. Rakhi, H.N. Alshareef, High energy density supercapacitors using macroporous kitchen sponges, Journal of Materials Chemistry, 22 (2012) 14394.
[29] Fu, G. Qi, R. Sahore, R. Sougrat, F.J. DiSalvo, E.P. Giannelis, Physical Chemistry Chemical Physics, 15 (2013) 19134-19137.
[30] L. Hu, H.S. Kim, J.-Y. Lee, P. Peumans, Y. Cui, Scalable coating and properties of transparent, flexible, silver nanowire electrodes, ACS Nano 4 (2010) 2955.
[31] Q. Cheng, Z. Song, T. Ma, B.B. Smith, R. Tang, H. Yu, H. Jiang, C.K. Chan, Nano Letters, 13 (2013) 4969.
[32] L. Hu, M. Pasta, F.L. Mantia, L. Cui, S. Jeong, H.D. Deshazer, J.W. Choi, S.M. Han, Y. Cui, Nano Letters, 10 (2010) 708.